

# The effect of RO oxides on microstructure and chemical durability of borosilicate glasses opacified by $P_2O_5$

M. Arbab, V.K. Marghussian\*, H. Sarpoolaky, M. Kord

*Ceramics Division, Department of Materials, Iran University of Science & Technology, Narmak, Tehran 16844, Iran*

Received 11 May 2005; received in revised form 31 October 2005; accepted 1 February 2006

Available online 4 May 2006

## Abstract

The microstructure, devitrification and chemical durability of borosilicate glass specimens opacified by  $P_2O_5$ , with the general composition  $SiO_2$  70,  $B_2O_3$  12,  $Al_2O_3$  2,  $P_2O_5$  2,  $Na_2O$  (13 –  $X$ ), RO  $X$  (wt.%) ( $R = Ca, Mg, Ba, Zn$ ) were investigated after being subjected to various heat treatment conditions, using DTA, XRD and SEM. It was shown that while heat treatments at 1073 K and  $>1123$  K were generally detrimental for the hydrolytic resistance of glasses, due to the enhanced phase separation or formation of excessive amounts of cristobalite, heating at 1123 K for 1 h usually improved the resistance due to the partial crystallization or microstructural changes of specimens. It was also found that a progressive decrease in hydrolytic and alkaline resistance occurred during prolonged heat treatment at 1123 K due to the formation of excessive amounts of cristobalite. It was also revealed that ZnO and MgO had the worst effect on chemical durabilities of specimens containing 7 and 5.5 wt.%  $Na_2O$ , respectively.

© 2006 Elsevier Ltd and Techna Group S.r.l. All rights reserved.

**Keywords:** B. Microstructure-final; C. Chemical properties; D. Glass; Opal glass

## 1. Introduction

Opals are essentially phase separated glasses, with their opacity resulting from light refraction and internal scattering between separated phases, which may be glassy or crystalline [1–3].

Phase separation may change many of properties of a glass, including chemical durability [4,5]. The microstructure is an important factor in these changes [6], e.g. when glass-in glass phase separation produces continuous immiscibility regions, leach paths for the least durable phase are continuous and usually an excessive degradation occurs in the glasses [4,6,7]. But opacification by minute crystals or after phase separation based on droplet shape regions of immiscibility, usually produces less durability problems [6,8,9].

Low thermal expansion phosphate opals are essentially borosilicate glasses [10,11]. Most of borosilicate glasses (including the commercial glasses) are phase separable [12]. A phase separated borosilicate glass, generally consists of a chemically durable (silica-rich) and a less durable borate rich phase. Many investigators have shown the effect of composition

and heat treatment on the phase separation mechanism, microstructure, and properties of borosilicate glasses [6,13–21].

It has also been shown that the addition of RO oxides ( $R = Ca, Mg, Ba, Zn \dots$ ) to borosilicate glasses, though is essential for enhanced opacity, by increasing the extent of phase separation [22], may generally be detrimental for chemical durability [23–25].

However, in spite of extensive research activities carried out and numerous publications existing in the above fields, it seems that relatively little comprehensive reports have appeared in literature concerning the effect of RO oxide additions on the microstructural changes and chemical durabilities of borosilicate glasses opacified by  $P_2O_5$ .

Therefore, in this study a systematic effort is made to show and compare the effect of CaO, MgO, BaO and ZnO additions on the chemical durability of low thermal expansion borosilicate glasses opacified by  $P_2O_5$ , with an emphasis on their microstructural changes. The composition of glasses studied were in the range of commercial low expansion opal glasses.

## 2. Experimental

In this study glass compositions were derived from a basic composition of glass N, in which RO oxides were substituted in

\* Corresponding author. Tel.: +98 21 77459151; fax: +98 21 77240480.

E-mail address: v\_k\_marghus@yahoo.com (V.K. Marghussian).

Table 1  
Chemical composition of glass specimens (wt.%)

| Specimen no.   | SiO <sub>2</sub> | Al <sub>2</sub> O <sub>3</sub> | B <sub>2</sub> O <sub>3</sub> | P <sub>2</sub> O <sub>5</sub> | Na <sub>2</sub> O | BaO | CaO | MgO | ZnO |
|----------------|------------------|--------------------------------|-------------------------------|-------------------------------|-------------------|-----|-----|-----|-----|
| N              | 71               | 2                              | 12                            | 2                             | 13                | –   | –   | –   | –   |
| B <sub>1</sub> | 71               | 2                              | 12                            | 2                             | 10                | 3   | –   | –   | –   |
| C <sub>1</sub> | 71               | 2                              | 12                            | 2                             | 10                | –   | 3   | –   | –   |
| M <sub>1</sub> | 71               | 2                              | 12                            | 2                             | 10                | –   | –   | 3   | –   |
| Z <sub>1</sub> | 71               | 2                              | 12                            | 2                             | 10                | –   | –   | –   | 3   |
| B <sub>2</sub> | 71               | 2                              | 12                            | 2                             | 7                 | 6   | –   | –   | –   |
| C <sub>2</sub> | 71               | 2                              | 12                            | 2                             | 7                 | –   | 6   | –   | –   |
| M <sub>2</sub> | 71               | 2                              | 12                            | 2                             | 7                 | –   | –   | 6   | –   |
| Z <sub>2</sub> | 71               | 2                              | 12                            | 2                             | 7                 | –   | –   | –   | 6   |
| B <sub>3</sub> | 71               | 2                              | 12                            | 2                             | 5.5               | 7.5 | –   | –   | –   |
| C <sub>3</sub> | 71               | 2                              | 12                            | 2                             | 5.5               | –   | 7.5 | –   | –   |
| M <sub>3</sub> | 71               | 2                              | 12                            | 2                             | 5.5               | –   | –   | 7.5 | –   |
| Z <sub>3</sub> | 71               | 2                              | 12                            | 2                             | 5.5               | –   | –   | –   | 7.5 |

1.5–3 wt.% steps for Na<sub>2</sub>O. Table 1 shows the chemical composition of glass specimens.

The series 1 specimens later were omitted from the research program, due to their relatively weak opacification tendencies and high thermal expansion coefficients.

Raw materials used were high quality commercial silica (Setabran Iran Glass Sand Corp. SA10 code) and AR grade H<sub>3</sub>BO<sub>3</sub>, Na<sub>2</sub>CO<sub>3</sub>, Al(OH)<sub>3</sub>, H<sub>3</sub>PO<sub>4</sub>, BaCO<sub>3</sub>, ZnO and Mg(OH)<sub>2</sub>. Glass batches were weighed, dry mixed in 100 g quantities and melted in an electric furnace at 1723–1823 K for 1 h using alumina crucibles. The melts were poured into preheated stainless steel moulds, transferred to an annealing furnace and annealed at 873 K for 1 h.

The thermal behavior of the glasses were followed by differential thermal analysis (DTA) at a heating rate of 20 K min<sup>−1</sup>, using alumina as an inert reference material. The glass specimens were heat treated for 1, 3, 5 and 7 h at their respective DTA exo-peak temperatures. The heating rate was chosen as 5 K min<sup>−1</sup> to minimize the deformation of specimens.

Samples of glasses in the as annealed condition and after heat treatment, were analyzed by X-ray diffractometry (XRD) to identify the crystalline phases.

The ISO procedures, designated as 719–1985E [26] and 695–1991E [27] were used for determining the chemical durability of the glasses in water and alkaline solutions, respectively. In the water resistance test the amount of alkali released into the water at 368 K after 1 h immersion is determined by immediate titration with a dilute hydrochloric acid solution and in the alkaline resistance test the resistant is calculated by the loss in mass per unit area of the glass specimen after 3 h immersion in a boiling aqueous solution of equal volumes of sodium carbonate and sodium hydroxide.

The microstructural characteristics of specimens were examined by scanning electron microscopy (SEM). The samples were prepared by etching in 2% HF solution prior to gold coating.

### 3. Results and discussion

Figs. 1 and 2 show the DTA traces for series 2 and 3 glass specimens, respectively. It can be seen that all glasses exhibited

exothermic effects. The broad peaks demonstrate the relatively low crystallization rates in these glasses.

The glass samples were heat treated for differing time periods at the temperature range 1073–1183 K, obtained from the DTA traces.

Tables 2 and 3 exhibit the summary of the crystalline phases formed in the series 2 and 3 specimens, respectively, after different heat treatment times and temperatures.

It is known that introduction of the oxides CaO or ZnO into alkali borosilicate glasses reduces the melting temperature and viscosity, promoting glass-in glass phase separation [28]. Therefore, the opacification was easily developed in the heat treated samples [20]. On the other hand the glass-in glass phase separation often promotes the crystallization process in glasses [29]. On the other hand, both phase separation and crystallization affect the chemical durability of these glasses. The effect of addition of RO oxides on hydrolytic chemical

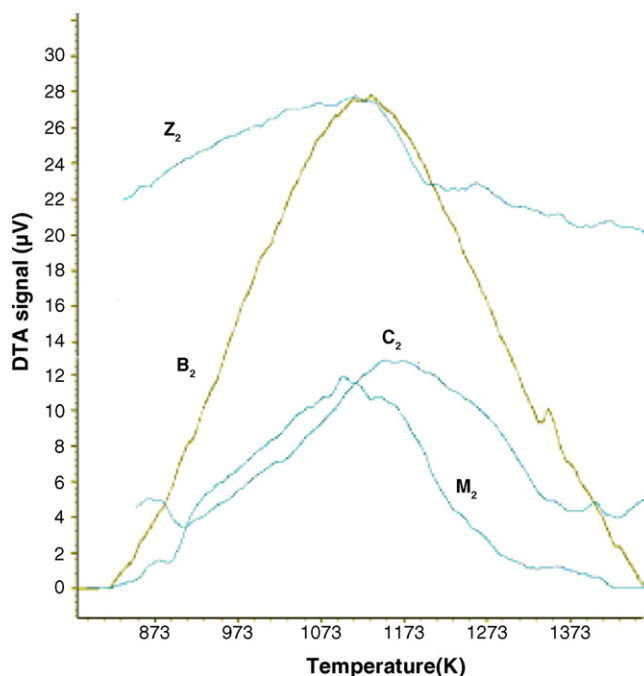


Fig. 1. DTA traces for series 2 specimens.

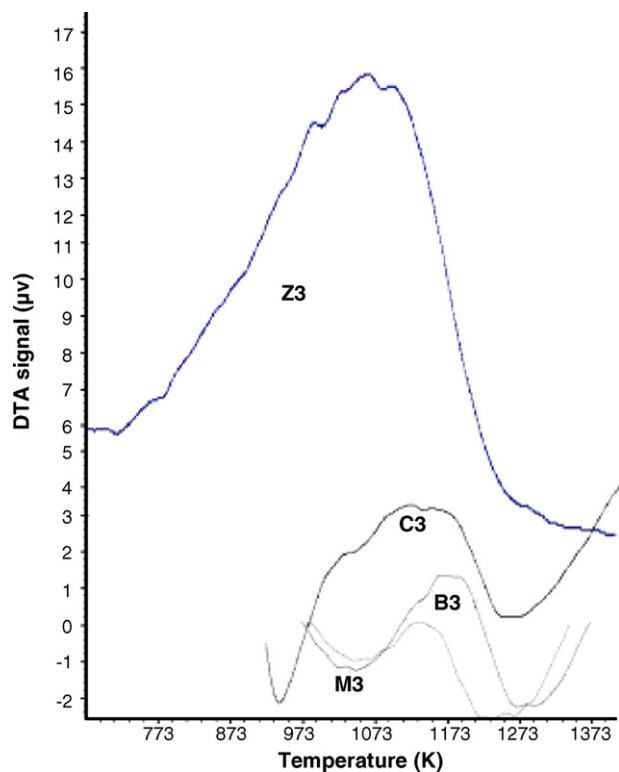


Fig. 2. DTA traces for series 3 specimens.

durability of series 2 glasses versus heat treatment temperature is shown in Fig. 3. It can be seen that the durability of glasses are usually decreased by heat treatment at 1073 K. This may primarily be attributed to the enhancement of glass-in glass phase separation process. The occurrence of this phenomenon is not detectable after annealing the glass specimens at 873 K, but some of them clearly show a quite advanced phase

Table 2  
Heat treatment conditions and crystallization products for series 2 specimens

| Specimen no.   | Heat treatment conditions (K h <sup>-1</sup> ) | Crystalline phases                                      |
|----------------|--|---|
| B <sub>2</sub> | 1123/1, 1158/1                                 | Cristobalite, Sodium barium phosphate                   |
| B <sub>2</sub> | 1123/3, 1123/5                                 | Cristobalite, Sodium barium phosphate, Barium phosphate |
| B <sub>2</sub> | 1123/7   | Cristobalite, Sodium barium phosphate                   |
| C <sub>2</sub> | 1123/1, 1158/1                                 | Cristobalite, Oxyapatite <sub>m</sub>                   |
| C <sub>2</sub> | 1123/3, 1123/5, 1123/7                         | Cristobalite, Oxyapatite <sub>m</sub>                   |
| Z <sub>2</sub> | 1123/1   | Cristobalite, Zinc phosphate                            |
| Z <sub>2</sub> | 1158/1   | Cristobalite  |
| Z <sub>2</sub> | 1123/3   | Cristobalite, Zinc phosphate                            |
| Z <sub>2</sub> | 1123/5, 1123/7                                 | Cristobalite  |
| M <sub>2</sub> | 1123/1   | Sodium magnesium phosphate                              |
| M <sub>2</sub> | 1158/1   | Cristobalite <sub>m</sub> , Sodium magnesium phosphate  |
| M <sub>2</sub> | 1183/1   | Cristobalite <sub>m</sub> , Sodium magnesium phosphate  |
| M <sub>2</sub> | 1123/3, 1123/5, 1123/7                         | Cristobalite, Sodium magnesium phosphate                |

m = the major phase.

Table 3

Heat treatment conditions and crystallization products for series 3 specimens

| Specimen no.   | Heat treatment conditions (K h <sup>-1</sup> ) | Crystalline phases                             |
|----------------|--|--|
| B <sub>3</sub> | 1123/1, 1158/1                                 | Cristobalite, Barium phosphate                 |
| B <sub>3</sub> | 1123/3, 1123/5, 1123/7                         | Cristobalite, Barium phosphate                 |
| C <sub>3</sub> | 1123/1   | Oxyapatite                                     |
| C <sub>3</sub> | 1158/1   | Cristobalite, Oxyapatite <sub>m</sub>          |
| C <sub>3</sub> | 1173/1   | Cristobalite, Oxyapatite <sub>m</sub>          |
| C <sub>3</sub> | 1223/1   | Cristobalite <sub>m</sub> , Oxyapatite         |
| C <sub>3</sub> | 1123/3, 1123/5                                 | Cristobalite, Oxyapatite <sub>m</sub>          |
| C <sub>3</sub> | 1123/7   | Cristobalite                                   |
| Z <sub>3</sub> | 1123/1, 1158/1                                 | Cristobalite, Sodium zinc phosphate            |
| Z <sub>3</sub> | 1123/3, 1123/5                                 | Cristobalite <sub>m</sub> , Zinc phosphate     |
| Z <sub>3</sub> | 1123/7   | Cristobalite                                   |
| M <sub>3</sub> | 1123/1, 1158/1                                 | Cristobalite, Magnesium phosphate <sub>m</sub> |
| M <sub>3</sub> | 1183/1, 1208/1                                 | Magnesium phosphate, Cristobalite              |
| M <sub>3</sub> | 1123/3   | Cristobalite                                   |
| M <sub>3</sub> | 1123/5, 1123/7                                 | Cristobalite, Sodium magnesium phosphate       |

m = the major phase.

separation after 1 h heat treatment at 1073 K. The specimen Z<sub>2</sub> containing 6 wt.% ZnO are the leading glass in this connection, also exhibiting the lowest resistance against water attack.

Fig. 4 shows the fine and continuous microstructure of separated phases in the above mentioned specimen indicating a possibly spinodal decomposition mechanism for phase separation.

Fig. 5 exhibits the EDX analysis of the glass after phase separation. It is clear that extensive phase separation has occurred in this glass leading to two distinctly different glass compositions one quite rich in SiO<sub>2</sub> (white regions in Fig. 4) and another rich in the remaining oxides.

The occurrence of an extensive microphase separation in these glasses can be explained by relatively high level of ionic potential ( $R = Z/r$ ) for Zn<sup>2+</sup> ions, where  $Z$  is the charge and  $r$  is the radius of ion. The extent of miscibility gap is correlated with the above mentioned ionic potential factor, varying according to the following sequence for alkaline earth ions [21,24]: Zn<sup>2+</sup>  $\approx$  Mg<sup>2+</sup> > Ca<sup>2+</sup> > Ba<sup>2+</sup>.

The difference in chemical durability observed between specimens M<sub>2</sub> (the second less durable) and Z<sub>2</sub> may be

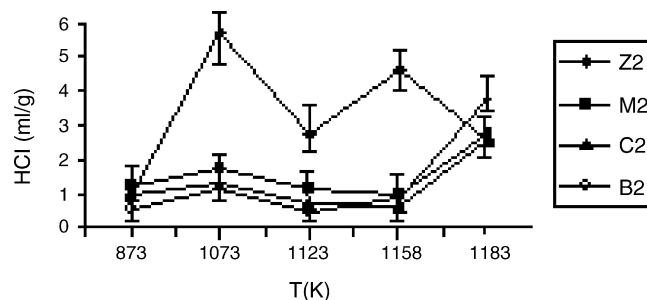


Fig. 3. Hydrolytic resistance of series 2 specimens as a function of heat treatment temperature, heat treatment time is 1 h.



Fig. 4. SEM micrograph of specimen Z<sub>2</sub> after heating at 1073 K for 1 h, showing an interconnected microphase separation (bar = 1 μm).

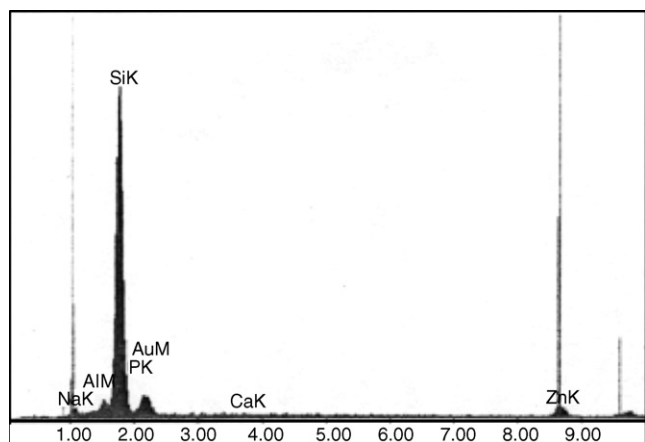


Fig. 5. EDX analysis of specimen Z<sub>2</sub> after heating at 1073 K for 1 h (the analysis of white regions in Fig. 4).

attributed to the higher interconnectivity and finer microstructure of specimen Z<sub>2</sub>.

Fig. 6 shows the microstructure of specimen M<sub>2</sub> heat treated under similar conditions (1073 K, 1 h).

Generally, the specimens exhibited improved resistance against water attack after being heat treated at higher temperature, e.g. 1123 K. This observation can be explained by the possibility of conversion of microstructures from a

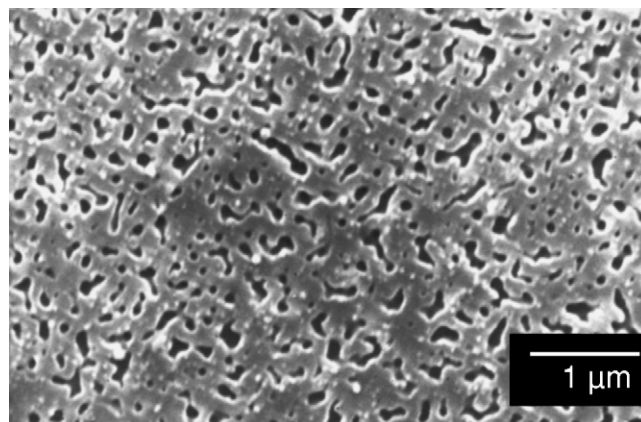


Fig. 6. SEM micrograph of specimen M<sub>2</sub> after heating at 1073 K for 1 h (bar = 1 μm).

continuous to a less continuous structure or even a microstructure containing isolated droplets embedded within a continuous phase (e.g. specimen Z<sub>2</sub> in Fig. 7) or appearance of some crystalline phases, having higher chemical durability in comparison to the initial glasses (e.g. specimen C<sub>2</sub>).

Fig. 8 depicts the microstructure of specimen C<sub>2</sub> showing tiny needle shape particles (mainly oxyapatite) without any sign of glass-in glass phase separation, giving rise to an improved resistance against water attack. This is consistent with the findings of other investigators [30,31].

Heating the specimens to higher temperatures in 1158–1183 K range, gave rise to a marked decrease in chemical durability in almost all of the specimens. This can be attributed to the increase of the amount of cristobalite phase and growing of its crystals to relatively large sizes that may lead to considerable stressing or even cracking of some specimens due to the well known  $\beta \rightarrow \alpha$  phase transformation, during cooling of specimens.

Fig. 9 shows an examples of highly cracked microstructure (specimens M<sub>2</sub>) after being heat treated at 1183 K for 1 h and Fig. 10 exhibits XRD pattern of the specimen showing the relatively high extent of cristobalite formation in this specimen.

Fig. 11 indicates the hydrolytic resistance of samples in series 2, after heat treating at 1123 K for differing time periods.

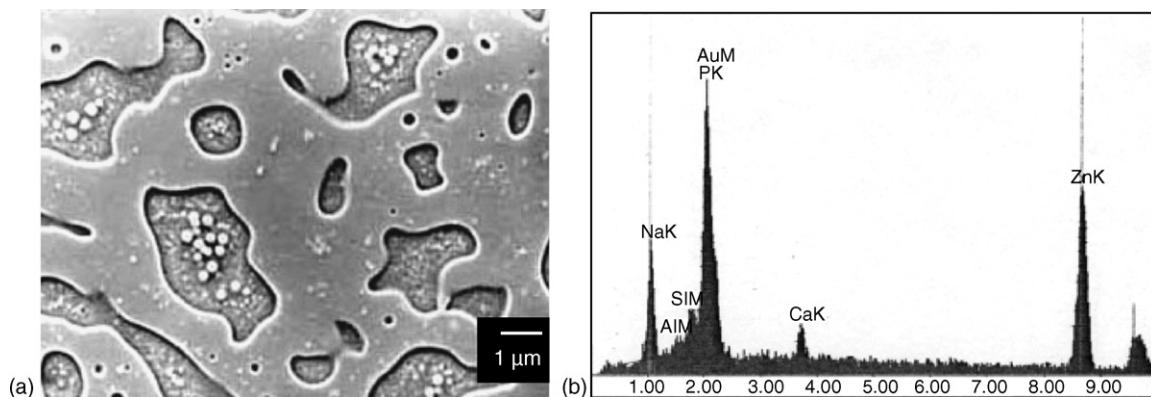


Fig. 7. SEM micrograph of specimen Z<sub>2</sub> after heating at 1123 K for 1 h: (a) showing zinc phosphate-rich droplets and secondary segregation of silica-rich particles within the drops (bar = 1 μm); (b) EDX analysis of the droplet phase.





Fig. 8. SEM micrograph of specimen C<sub>2</sub> after heating at 1123 K for 1 h, showing crystalline particles of oxyapatite (bar = 1 μm).

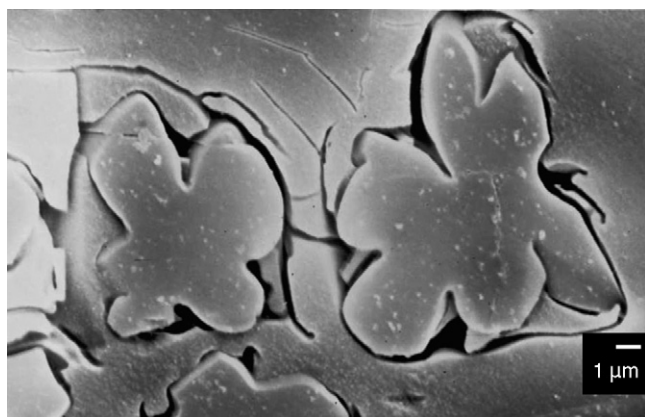


Fig. 9. SEM micrograph of specimen M<sub>2</sub> after heating at 1183 K for 1 h, showing a highly cracked microstructure (bar = 1 μm).

The curves show almost the same tendencies as explained before in connection to the effect of temperature. After 3 h all specimens except Z<sub>2</sub>, show relatively slight deterioration in durability. This can be explained by the enhanced phase separation, whereas in the case of specimens containing ZnO the improvement in durability can be attributed to the

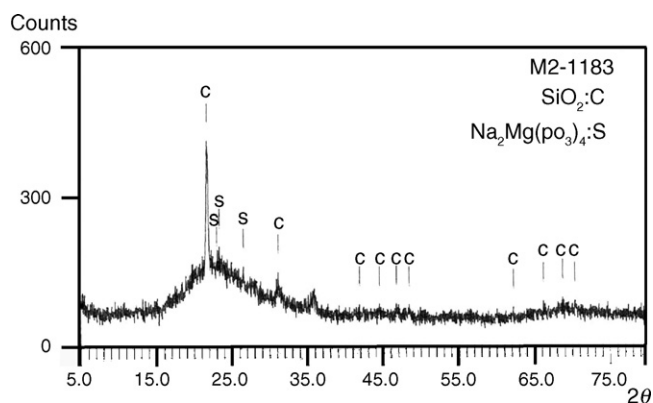


Fig. 10. XRD patterns of specimen M<sub>2</sub> crystallized at 1183 K for 1 h.

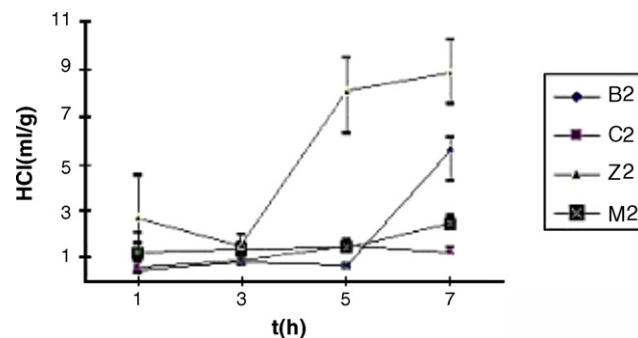


Fig. 11. Hydrolytic resistance of series 2 specimens as a function of heat treatment time, at 1123 K.

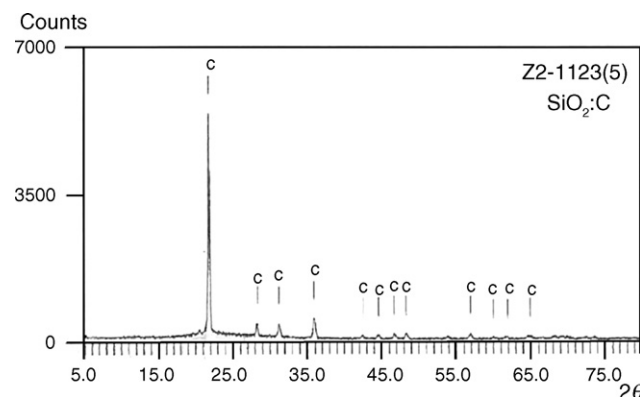


Fig. 12. XRD pattern of specimen Z<sub>2</sub> crystallized at 1123 K for 5 h.

occurrence of a relatively high degree of crystallization leading to formation of a zinc phosphate phase (Table 2). The latter specimen exhibits a quite high amount of cristobalite after 5 h heat treatment (Fig. 12 and Table 2), leading to highly cracked specimens and a marked drop in durability. Other specimens also show similar decrease in durability after prolonged heating at 1123 K due to the formation of high amounts of cristobalite and its extensive grain growth. One interesting exception is specimen C<sub>2</sub> containing CaO, which after prolong heat treatment mainly develops an apatite phase (Table 2) exhibiting a fine microstructure of interconnected fibers (Fig. 13).

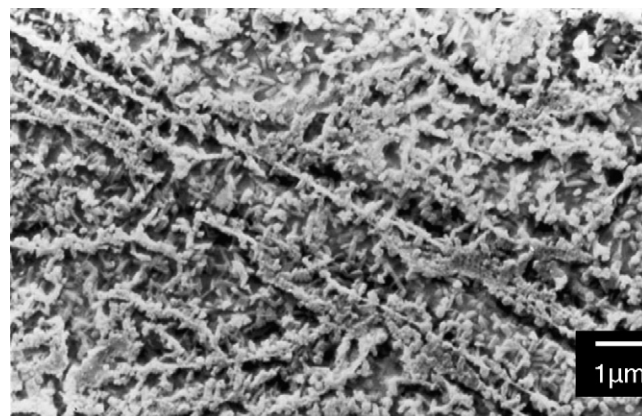


Fig. 13. SEM micrograph of specimen C<sub>2</sub> after heating at 1123 K for 5 h, showing a fine microstructure of interconnected fibers (bar = 1 μm).

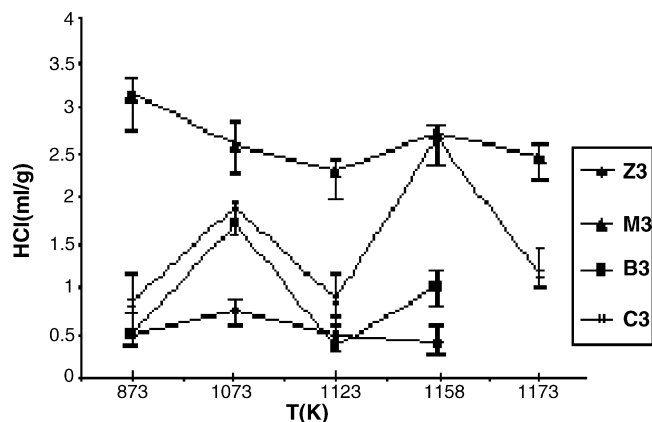


Fig. 14. Hydrolytic resistance of series 3 specimens as a function of heat treatment temperature, heat treatment time is 1 h.

In Fig. 14 are shown the hydrolytic resistance of the specimens in series 3. Except the specimen M<sub>3</sub> showing a continuous increase in durability upon the temperature elevation from 873 to 1123 K, other specimens behave almost similarly as specimens in series 2, namely a decreased durability due to the enhanced phase separation followed by an increase due to the crystallization or microstructural change from a continuous to a discontinuous structure and finally a marked decrease due to the excessive formation and growth of cristobalite crystals. In the case of specimen M<sub>3</sub>, it can be suggested that this specimen probably has extensively been phase separated even after annealing at 873 K. The relatively low resistance against water attack in this specimen is an evidence for this deduction, although such phase separation was not detectable in the specimen by SEM.

Fig. 15 shows the microstructure of specimen M<sub>3</sub> after 1 h heating at 1073 K. It seems that the relatively coarse microstructure that has just begun to neck off and form isolated phases is responsible for enhanced durability in this specimen. Fig. 16 depicts the microstructure of the same specimen after being heated up for 1 h at 1123 K showing the

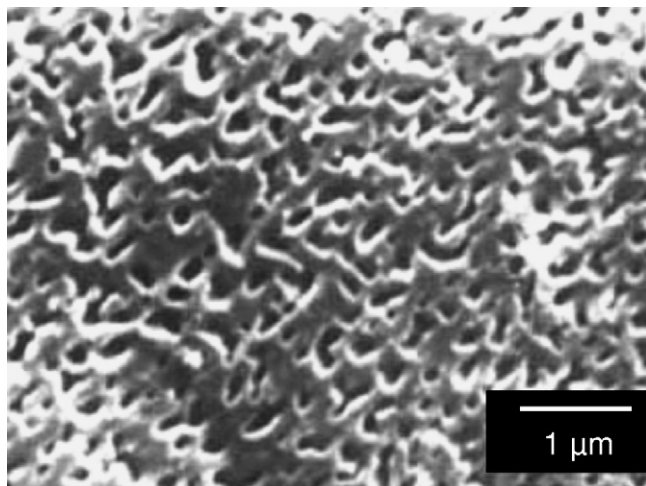


Fig. 15. SEM micrograph of specimen M<sub>3</sub> after heating at 1073 K for 1 h (bar = 1 μm).

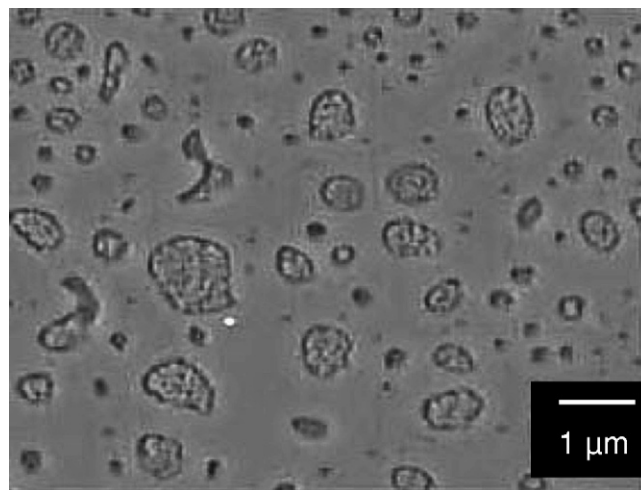


Fig. 16. SEM micrograph of specimen M<sub>3</sub> after heating at 1123 K for 1 h, showing magnesium phosphate-rich droplets and secondary segregation of silica-rich particles within the drops (bar = 1 μm).

droplet phase and the occurrence of secondary phase separation and some crystallization improving the durability.

Fig. 17 shows the variation of hydrolytic durability of the series 3 specimens versus heat treatment time at 1123 K.

It seems that all specimens show a more or less constant durability for 1–3 h after which a considerable deterioration occurred, especially >5 h due to the extensive formation of cristobalite. The specimen M<sub>3</sub> is an exception exhibiting a marked decrease in durability after 3 h followed by a considerable increase after 5 h. This again can be attributed to the formation of excessive amounts of cristobalite after 3 h and its partial dissolution in the glassy phase or its conversion to magnesium phosphate after 5 h in this specimen (see Table 3). Fig. 18 depicts the microstructure of the above-mentioned specimen after 3 h heating at 1123 K.

Figs. 19 and 20 illustrate the chemical resistance of series 2 and 3 specimens to the standard alkaline solution attack, respectively.

As can be seen from Fig. 19 all series 2 glasses after a 3 h heat treatment at 1123 K, show a slight increase in chemical durability which can be attributed to the partial crystallization of all specimens, whereas the relative drop in durability occurring later can be related to the formation of cristobalite

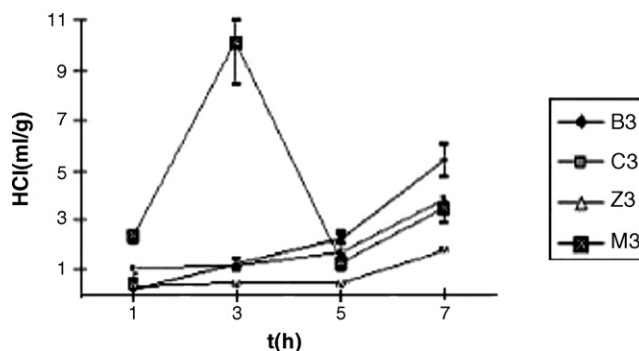


Fig. 17. Hydrolytic resistance of series 3 specimens as a function of heat treatment time, at 1123 K.

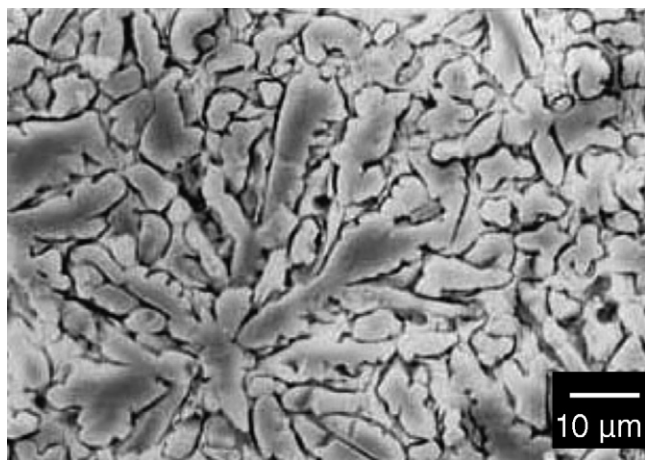


Fig. 18. SEM micrograph of specimen M<sub>3</sub> after heating at 1123 K for 3 h, showing the extensive formation of cristobalite (bar = 10 μm).

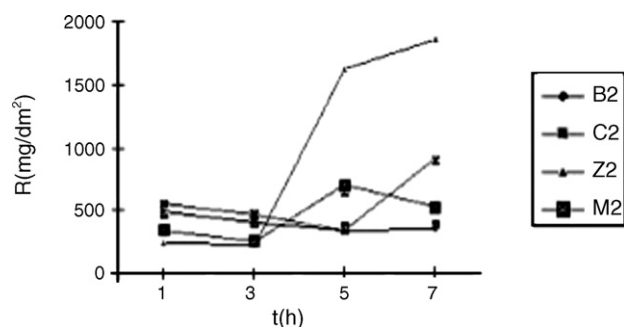


Fig. 19. Alkaline resistance of series 2 specimens as a function of heat treatment time, at 1123 K.

which is quite distinct after 7 h especially in some specimens like Z<sub>2</sub> (see Fig. 12 and Table 2).

In the case of series 3 specimens (Fig. 20) similar deductions can be made. In this case the specimen M<sub>3</sub> shows a relatively larger variation in durability. This behavior can be attributed to the occurrence of a severe crystallization process leading to the formation of cristobalite after 3 h and its dissolution and conversion to phosphate phases after longer times, as described before.

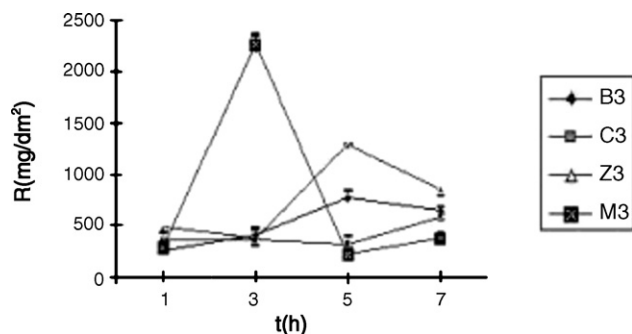


Fig. 20. Alkaline resistance of series 3 specimens as a function of heat treatment time, at 1123 K.

#### 4. Conclusions

It was shown that chemical durability of the chosen alkaline borosilicate glasses opacified by P<sub>2</sub>O<sub>5</sub>, is highly dependent on the amount and type of RO oxides used and the temperature and time of heat treatment.

The hydrolytic durability generally deteriorates by heat treating the specimens for 1 h at the temperature of 1073 K and 1123–1183 K range and times exceeding 3 h at 1123 K. The intensification of glass-in glass phase separation and formation of cristobalite, in high quantities and large crystal sizes, are the main causes for the above observations. But heat treating the specimens at 1123 K for 1 h generally improves the durability due to the modification of the structural characteristics of the phase separated phases from continuous to isolated and partial crystallization of specimens. While the use of ZnO in series 2 specimens (containing 6 wt.% RO) has the most detrimental effect on chemical durability of these glasses, the glasses containing CaO generally show the highest chemical durability due to the formation of apatite crystals.

In the series 3 specimens (containing 7.5 wt.% RO) the specimens containing MgO are generally the most vulnerable specimens to water attack, while contrary to the series 2 specimens, the specimens containing ZnO, show a relatively good resistance to water attack.

While the resistance of both series of specimens to alkali attack, after being heat treated at 1123 K for <3 h, is good and nearly constant and independent to composition, it deteriorates and becomes highly time and composition dependent for longer heat treatment times. The specimens containing ZnO show the least resistance to alkali attack after soaking at 1123 K for >5 h in both series of specimens.

The role of P<sub>2</sub>O<sub>5</sub> is more complicated. It seems that addition of this oxide have diverse effects on chemical durability. In one hand, in some conditions it can intensify the phase separation process (due to its relatively high ionic field strength) and on the other hand, in some cases it could be responsible for formation of phosphate phases (like apatite and zinc or magnesium phosphates) which generally improve the chemical durability.

#### References

- [1] J.E. Flannery, D.R. Wexell, in: D.C. Boyd, J.F. MacDowell (Eds.), *Opal Glasses in Commercial Glasses*, American Ceramic Society, Columbus, OH, 1986, pp. 141–150.
- [2] S.J. Schneider, *Engineered Materials. Hand Book of Ceramic and Glasses*, vol. 4, ASM, 1991 Technical Chairman, p. 1101.
- [3] W. Vogel, *Chemistry of Glass*, The American Ceramic Society, Columbus, OH, 1985, p. 196.
- [4] O.V. Mazurin, E.A. Porai-Koshits, *Phase Separation in Glass*, Elsevier, North-Holland, 1984, pp. 269–275.
- [5] W. Vogel, *The Structure of Opalescent Sodium-Borosilicate Glasses in Structure and Crystallization of Glasses*, Pergamon Press, Oxford, 1971, pp. 75–76.
- [6] P. Taylor, S.D. Ashmore, D.J. Owen, Chemical durability of some sodium borosilicate glasses improved by phase separation, *J. Am. Ceram. Soc.* 70 (1987) 333–338.
- [7] J.E. Flannery, Chemical durable phosphate opal glasses, U.S. Patent 4309218, 5 January 1982.

- [8] W. Vogel, Chemistry of Glass, Columbus, the American Ceramic Society, Columbus, OH, 1985, p. 199.
- [9] J.E. Flannery, W.H. Dumbaugh, G.B. Carrier, Improving the opacity of phase-separated opal glasses by alterations of the interfacial tension, *Am. Ceram. Soc. Bull.* 54 (1975) 1066–1068 (Continued on page 1071).
- [10] M.B. Volf, Technical Approach to Glass, Elsevier, New York, 1990 p. 255.
- [11] E.C. Hagedorn, Opalizable glass compositions, U.S. patent 3764283, 9 October, 1973.
- [12] W. Vogel, The Structure of Opalescent Sodium-Borosilicate Glasses in Structure and Crystallization of Glasses, Pergamon Press, Oxford, 1971, pp. 66–68.
- [13] R.J. Charles, Phase separation in borosilicate glasses, *J. Am. Ceram. Soc.* 47 (1964) 559–563.
- [14] W. Haller, D.H. Blackburn, F.E. Wagstaff, R.J. Charles, Metastable immiscibility surface in the system  $\text{Na}_2\text{O}-\text{B}_2\text{O}_3-\text{SiO}_2$ , *J. Am. Ceram. Soc.* 53 (1970) 34–39.
- [15] B.F. Howell, J.H. Simmons, W. Haller, Loss of chemical resistance to aqueous attack in a borosilicate glass due to phase separation, *Am. Ceram. Soc., Bull.* 54 (1975) 707–709.
- [16] T. Takamori, M. Tomozawa, HCl leaching rate and microstructure of phase separated borosilicate glasses, *J. Am. Ceram. Soc.* 61 (1978) 507–512.
- [17] T. Takamori, M. Tomozawa, Viscosity and microstructure of phase separated borosilicate glasses, *J. Am. Ceram. Soc.* 62 (1979) 373–377.
- [18] P. Taylor, D.J. Owen, Liquid immiscibility in the system  $\text{Na}_2\text{O}-\text{ZnO}-\text{B}_2\text{O}_3-\text{SiO}_2$ , *J. Am. Ceram. Soc.* 64 (1981) 360–367.
- [19] G. Perera, R.H. Duremus, Dissolution rates of commercial soda-lime and pyrex borosilicate glasses: influence of solution PH, *J. Am. Ceram. Soc.* 74 (1991) 1554–1558.
- [20] S.N. Salama, S.M. Salama, H. Darwish, Crystallization characteristics of some lithia calcia magnesia borosilicate glasses, *Ceram. Int.* 21 (1995) 159–167.
- [21] P. Taylor, A.B. Campbell, D.G. Owen, Liquid immiscibility in the system  $\text{X}_2\text{O}-\text{MO}-\text{B}_2\text{O}_3-\text{SiO}_2$  ( $\text{X} = \text{Na}, \text{K}$ ;  $\text{M} = \text{Mg}, \text{Ca}, \text{Ba}$ ) and  $\text{Na}_2\text{O}-\text{MgO}-\text{BaO}-\text{B}_2\text{O}_3-\text{SiO}_2$ , *J. Am. Ceram. Soc.* 66 (1982) 347–351.
- [22] M.B. Volf, Technical Approach to Glass, Elsevier, New York, 1990, pp. 257–258.
- [23] W. Vogel, Chemistry of Glass, the American Ceramic Society, Columbus, OH, 1985, pp. 199–204.
- [24] O.V. Mazurin, E.A. Porai-Koshits, Phase Separation in Glass, Elsevier, North-Holland, 1984, pp. 132–134.
- [25] M.B. Volf, Chemical Approach to Glass, Elsevier, New York, 1984, p. 267.
- [26] International Standards organization, Determination of the Hydrolytic Resistance of Glass Grains at 98 °C, I.S.O, 1985,, p. 719.
- [27] International Standards organization, Determination of the Resistance of Glassware to Attack by a Boiling Aqueous Solution of Mixed Alkali, I.S.O, 1985,, p. 695.
- [28] V.Kh. Nikulin, O.S. Viktorova, L.M. Prusakova, R.I. Ainetdinova, M.G. Meshcheryakova, Effect of liquidation on the properties of low-alkali-borosilicate glasses, *Glass Ceram.* 48 (1991) 145–150.
- [29] W.D. Kingery, H.K. Bowen, D.R. Uhlmann, Introduction to Ceamics, John Wiley and Sons, New York, 1976, pp. 368–369.
- [30] S.J. Schneider, Engineered Materials, Hand Book of Ceramic and Glasses, 4, ASM, 1991 (Technical Chairman, p. 1011).
- [31] R.Z.Le. Geros, Calcium phosphate materials in restorative dentistry: a review, *Adv. Dent. Res.* 2 (1988) 164–180.